SCIENTIFIC REP🛞RTS

OPEN

Highly Efficient and Stable Solar Cells Based on Thiazolothiazole and Naphthobisthiadiazole Copolymers

Masahiko Saito[1,2], Itaru Osaka[2,3], Yasuhito Suzuki[2], Kazuo Takimiya[1,2], Takashi Okabe[4], Satoru Ikeda[4] & Tsuyoshi Asano[4]

A critical issue in polymer-based solar cells (PSCs) is to improve the power conversion efficiency (PCE) as well as the stability. Here, we describe the development of new semiconducting polymers consisting of thiophene, thiazolothiazole and naphthobisthiadiazole in the polymer backbone. The polymers had good solubility and thus solution-processability, appropriate electronic structure with narrow band gaps of ~1.57 eV and low-lying HOMO energy levels of ~−5.40 eV, and highly ordered structure with the favorable face-on backbone orientation. Solar cells based on the polymers and $PC_{71}BM$ exhibited quite high PCEs of up to 9%. More interestingly, the cells also demonstrated excellent stability as they showed negligible degradation of PCE when stored at 85 °C for 500 hours in the dark under nitrogen atmosphere. These results indicate that the newly developed polymers are promising materials for PSCs in the practical use.

Bulk heterojunction (BHJ) solar cells composed of semiconducting polymers as p-type and fullerene derivatives as n-type materials (PSCs) are of great interest as flexible and large-area renewable energy sources that can be produced by solution-processes[1–3]. A number of semiconducting polymers have been developed in the last decade, which have brought about significant improvement in the power conversion efficiency (PCEs)[4–8]. More recently, optimization of processing methods and device structures by using such polymers have led to the further improvement of PCEs reaching 10%[9–13].

Important structural features desired for semiconducting polymers are well-ordered π–π stacking structure and "face-on" backbone orientation, where the backbone plane lies flat on a substrate, which facilitates the charge carrier transport along the film thickness[14]. In parallel, polymers are required to have a wide absorption range, namely a narrow band gap, to absorb as much sunlight as possible, which gives rise to the high short-circuit current density (J_{SC}). They also need to have a low-lying highest occupied molecular orbital (HOMO) energy level to maximize the open-circuit voltage (V_{OC}) that is proportional to the energy difference between HOMO of the semiconducting polymer and the lowest unoccupied molecular orbital (LUMO) of the fullerene derivative[15,16]. To fulfill these requirements, donor-acceptor (D-A) polymers consisting of an electron-rich unit (donor; D) and an electron-poor unit (acceptor; A) have been widely investigated[17–20].

Recently, we have reported that a D-A copolymer system based on alkylthiophenes and thiazolothiazole (TzTz)[21–26] as the D and A units, respectively (PTzBTs, Fig. 1), showed relatively high PCEs of

[1]Department of Applied Chemistry, Graduate School of Engineering, Hiroshima University, 1-4-1 Kagamiyama, Higashi-Hiroshima, Hiroshima, 739-8527, Japan. [2]Emergent Molecular Function Research Group, RIKEN Center for Emergent Matter Science, Wako, Saitama 351-0198, Japan. [3]Precursory Research for Embryonic Science and Technology (PRESTO), Japan Science and Technology Agency, Chiyoda-ku 102-0075 Japan. [4]Central Technical Research Laboratory, JX Nippon Oil & Energy Corporation, 8, Chidoricho, Naka-ku, Yokohama 231-0815, Japan. Correspondence and requests for materials should be addressed to I.O. (email: itaru.osaka@riken.jp)
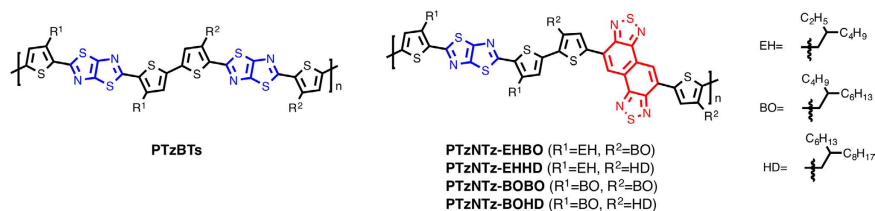
Figure 1. Chemical structure of semiconducting polymers based on thiophene and thiazolothiazole (PTzBTs), and thiophene, thiazolothiazole and naphthobisthiadiazole (PTzNTzs).

Polymer	M_n (kDa)	M_w (kDa)	PDI	E_{HOMO} (eV)		E_{LUMO} (eV)[b]	λ_{max} (nm)	λ_{edge} (nm)/E_g^{opt} (eV)[d]
				CV[b]	PESA[c]			
PTzNTz-EHBO	32.7	64.3	2.0	−5.41	−5.28	−3.45	490, 643, 677	784/1.58
PTzNTz-EHHD	47.0	91.8	2.0	−5.40	−5.28	−3.46	487, 633, 675	787/1.58
PTzNTz-BOBO	51.6	113.2	2.2	−5.40	−5.30	−3.46	482, 678	791/1.57
PTzNTz-BOHD	29.1	59.2	2.2	−5.41	−5.29	−3.44	477, 680,	788/1.57

Table 1. Polymerization results[a] and electronic properties of the polymers. [a]Determined by high temperature GPC (DCB, 140 °C) using polystyrene standard. [b]HOMO and LUMO energy levels determined by cyclic voltammetry. [c]HOMO energy levels evaluated by photoelectron spectroscopy in air (PESA). [d]λ_{edge}: absorption edge, E_g: optical band gap.

~7.5% in conventional cells[27,28]. The high performance most likely originates in the ordered and close π−π stacking structure as well as the face-on orientation. Although PTzBTs have low HOMO energy levels of ca. −5.2 eV resulting in high V_{OC}s of ~0.9 V in solar cells, their relatively wide band gap of 1.8 eV, *i.e.*, absorption range of up to 675 nm, limited J_{SC}s to ~13 mA cm^{−2}. Thus, for the further improvement of PCE the band gap of PTzBTs must be narrowed while maintaining or even lowering the HOMO energy level. In order to realize such electronic structure, a more electron-poor unit, *i.e.*, a stronger A unit, should be introduced into the backbone.

In this work, we report on a D-A polymer system incorporating naphthobisthiadiazole (NTz)[6,14,29–32] as the stronger A unit in addition to the thiophene-TzTz backbone (PTzNTzs, Fig. 1). As NTz is a rigid and π−extended fused ring, the new polymer system is expected to have a well-ordered π−π stacking structure as well as an appropriate electronic structure as mentioned above. We describe the synthesis, electronic structure, and ordering structures of PTzNTzs and their solar cell performances. We also note that, interestingly, the solar cells based on PTzNTzs showed excellent thermal stability compared to the cells based on PTzBTs.

Results

All polymers were synthesized via the Stille coupling reaction using the stannylated TzTz monomers with the 2-ethylhexyl group (EH) or the 2-butyloctyl group (BO) on the thiophene rings as R^1 (1a-1b) and the brominated NTz monomers with BO and the 2-hexyldecyl group (HD) on the thiophene rings as R^2 (2a-2b) (Scheme S1). Thus, PTzNTz with four different side chain combinations were synthesized (PTzNTz-EHBO, -EHHD, -BOBO, -BOHD). The solubility was significantly different between PTzNTz-EHBO and others; whereas PTzNTz-EHBO was soluble in hot chlorobenzene (CB), or *o*-dichlorobenzene (DCB), PTzNTz-EHHD, −BOBO, and −BOHD was soluble even in chloroform (CF), CB and DCB below ca. 40 °C. Interestingly, the solubility of PTzNTzs was improved compared with PTzBTs despite the fact that NTz with a more π−extended ring than TzTz was introduced into the backbone. For example, in order to prepare a 5 g/L solution in CB, whereas PTzBT-BOHD required heating at around 100 °C, PTzNTz-BOHD, with the same side chain combination, did not require heating. The number-average molecular weight (M_n), evaluated by GPC at 140, of PTzNTz-EHBO, -EHHD, -BOBO and -BOHD were about 30–50 kDa with the polydispersity index (PDI) of around 2 (Table 1). Thermal property of the polymers was studied by differential scanning calorimetry (DSC). It was revealed that whereas PTzNTz-EHHD, -BOBO and -BOHD showed transition peaks between 250–300 °C, PTzNTz-EHBO did not show transition peaks below 350 °C (Figure S6). This implies that PTzNTz-EHBO has a more rigid structure and strong aggregation nature than the others most likely due to the shorter alkyl side chains, which seemingly correlate with the solubility difference.

The HOMO energy level (E_{HOMO}) and the LUMO energy level (E_{LUMO}) of the polymers were evaluated by cyclic voltammetry (Fig. 2a) using the polymer thin films. All the polymers showed similar
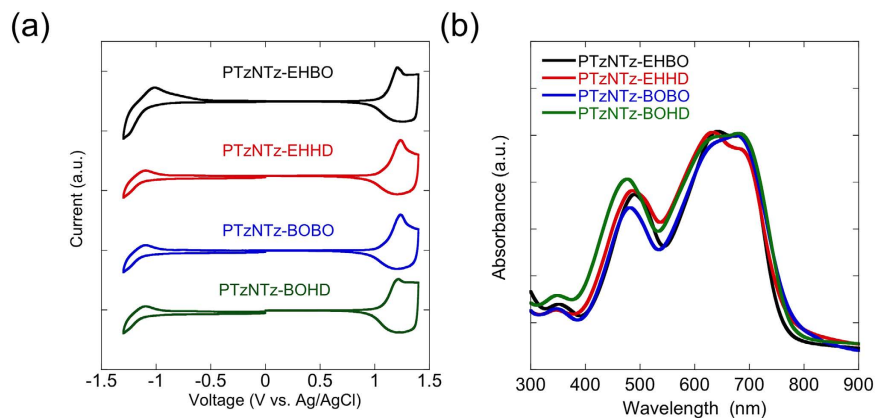
Figure 2. Cyclic voltammograms (a) and UV-vis absorption spectra (b) of the polymer thin films.

voltammograms, suggesting that the effect of the side chain is negligible. The oxidation and reduction onset potentials were about 1.07–1.08 V and -0.89–-0.91 V, respectively, which correspond to E_{HOMO} of -5.40–-5.41 eV and E_{LUMO} of -3.44–-3.46 eV (Table 1). As expected from the introduction of the strong acceptor unit NTz, E_{HOMO}s of PTzNTzs (ca. -5.40 eV) were lower than those of PTzBTs (ca. -5.31 eV, Table S2). The downward shift of E_{LUMO} from PTzBTs (-3.25 eV, Table S2) to PTzNTz was more pronounced than that of E_{HOMO}, which is natural because, in general, the acceptor unit affects more on LUMO than HOMO[33]. E_{HOMO} was also evaluated by photoelectron spectroscopy in air (PESA). E_{HOMO} was around -5.30 eV, which was lower by ca. 0.1 eV than that of PTzBTs, which is consistent with the results obtained from CV.

Figure 2b displays the UV-vis absorption spectra of the polymers in the thin film. All the polymers exhibited similar spectra with the absorption range of 400–800 nm. The absorption maximum (λ_{max}) was ca. 680 nm (Table 1), which was red-shifted from that of PTzBTs by 60 nm. The absorption edge (λ_{edge}) was determined to be ca. 790 nm, which corresponds to the optical band gap (E_g) of 1.57–1.58 eV (Table 1). These values were about 0.2 eV smaller than that of PTzBTs. Thus, as expected from the molecular design, PTzNTzs have both the narrower Eg and lower E_{HOMO} than PTzBTs.

The ordering structure of the polymers was investigated by the X-ray diffraction studies[34]. Two-dimensional grazing incidence X-ray diffraction (2D GIXD) images of the polymer-only films and the polymer/[6,6]-phenyl-C_{71}-butyric acid methyl ester (PC$_{71}$BM) blend films on the indium tin oxide (ITO)/ZnO substrate are shown in Fig. 3. In the polymer-only films (Fig. 3a), a diffraction corresponding to the π–π stacking structure ($q \approx 1.65$–1.70 Å^{-1}) clearly appeared on the q_z axis for PTzNTz-EHBO and -BOBO, indicating that they formed crystalline domains with a favorable face-on orientation. The π–π stacking distances (d_π) of these polymers were 3.69 and 3.72 Å, respectively (Figure S8, Table S3). In the meantime, the π–π stacking diffraction for PTzNTz-EHHD and -BOHD appeared very weak and d_π was wider for PTzNTz-EHHD and -BOHD with 3.77 and 3.80 Å, respectively (Figure S8, Table S3), indicating that the crystallinity was low. The difference in d_π indicates that, in this system, the use of the HD group as the side chain diminishes the intermolecular interaction. It is also noted that these d_π values are wider than that of PTzBTs (3.5 Å), even though NTz is a more π–extended fused ring and thus is expected to enhance the π–π stacking. This can be explained by the difference in the placement of the alkyl groups. In PTzBTs, all the alkyl groups on the thiophene rings point toward TzTz. In PTzNTzs, on the other hand, whereas the alkyl groups on the thiophene rings neighboring TzTz point toward TzTz, those neighboring NTz point outward from NTz. The *less* regularly placed alkyl groups as such in PTzNTzs compared to the regularly placed alkyl groups in PTzBTs could somehow weaken the π–π interaction. The difference of crystallinity between PTzNTzs and PTzBTs apparently correlates to the difference of solubility. In addition, in particular, when the alkyl groups are longer than those of PTzNTz-EHBO, the interaction becomes weaker and in turn the solubility becomes significantly higher.

In the polymer/PC$_{71}$BM blend films fabricated from CB solutions (Fig. 3c), only PTzNTz-EHBO showed a clear π–π stacking diffraction along the q_z axis. d_π was unchanged by blending with PC$_{71}$BM. The PTzNTz-BOBO blend film also showed a π–π stacking diffraction, but the intensity was quite weak. The results in the blend films are consistent with those in the polymer-only films. In contrast, when 1,8-diiodooctane (DIO) was used for the film fabrication as the solvent additive[35], all the polymers exhibited a diffraction corresponding to the π–π stacking of face-on crystallites (Fig. 3d), indicating that the ordering structure was enhanced particularly for PTzNTz-EHHD, -BOBO, and -BOHD. The different behavior between PTzNTz-EHBO and the others in the DIO-aided films can be explained as follows. In the case of PTzNTz-EHHD, -BOBO, and -BOHD, with the higher solubility and thus weaker aggregation nature, the addition of DIO may slow down the crystallization of PC$_{71}$BM, during which time the polymers crystallize as typically seen for many polymers[36]. It is also noted that the addition of DIO even enhances the crystallization of PTzNTz-EHHD, -BOBO, and -BOHD in the polymer-only films
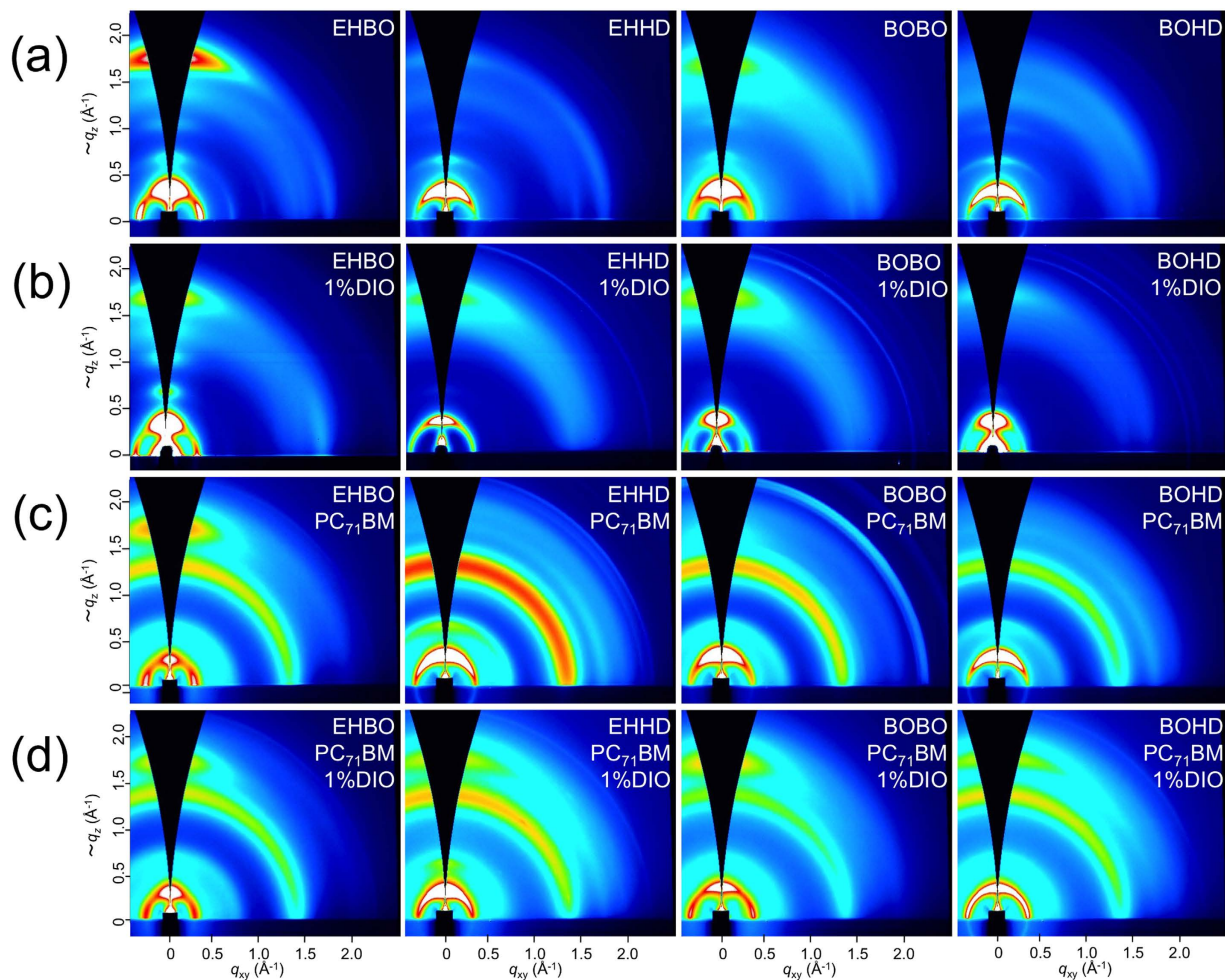
Figure 3. 2D GIXD patterns of polymer-only films **(a)**, DIO (1%)-aided polymer-only films **(b)**, polymer/PC$_{71}$BM blend films **(c)**, and DIO (1%)-aided polymer/PC$_{71}$BM blend films **(d).** The alkyl groups are shown at the right top of each image.

(Fig. 3b), as the $\pi-\pi$ stacking diffraction appeared clear and the lamellar diffraction appeared as spot-like compared to the polymer-only films without DIO. In contrast, in the case of PTzNTz-EHBO, due to the strong aggregation nature and thus the lower solubility, it well crystallizes regardless of the addition of DIO (regardless of the crystallization speed of PC$_{71}$BM). The improved ordering structures are consistent with the solar cell performances as shown below.

We investigated the surface morphology of the polymer/PC$_{71}$BM blend films by the atomic force microscopy (AFM) (Fig. 4). In the blend films fabricated with CB (Fig. 4a), whereas the PTzNTz-EHBO film formed well phase-separated morphologies, which would enlarge the polymer/PC$_{71}$BM interface area and thus ensure the charge separation, other polymers, in particular PTzNTz-BOBO and -BOHD, formed large domains that is detrimental to the charge separation. In the DIO-aided blend films (Fig. 4b), on the other hand, whereas no morphological change was observed for PTzNTz-EHBO, drastic improvement of the morphology was observed for other polymers. These results are also in good agreement with the solar cell performances of the polymers as described below.

Solar cells with an inverted structure, ITO/ZnO/active layer/MoO$_x$/Ag, were used to investigate the photovoltaic properties of the polymers. PC$_{71}$BM was used as the n-type material, and the active layer was fabricated from the CB solution. The optimal polymer to PC$_{71}$BM weight ratio was 1:1.5 for all polymers. The current density (J)-voltage (V) curves and the external quantum efficiency (EQE) spectra of the cells under 1 sun of simulated AM 1.5G solar irradiation (100 mW/cm^2) are displayed in Fig. 5a,b, respectively. The photovoltaic parameters are summarized in Table 2. All the cells showed similar V_{OC} of 0.84–0.85 V. Although E_{HOMO} of PTzNTzs was lower than that of PTzBT by 0.1 eV, V_{OC}s of the PTzNTzs cells were slightly decreased by 0.03–0.04 V. The origin of the energetic loss is yet unknown. The PTzNTz-EHBO cells gave relatively high J_{SC} of ~16.0 mA cm^{-2} compared to that of the PTzBT cells (~13 mA cm^{-2})[28]. This is mainly due to the wider spectral response of the PTzNTz-EHBO cell covering 400–800 nm as seen in the EQE spectrum. Interestingly, the cells using PTzNTz-EHHD, -BOBO, and -BOHD exhibited significantly lower J_{SC} of around 2–4 mA cm^{-2}, which is consistent with the EQE
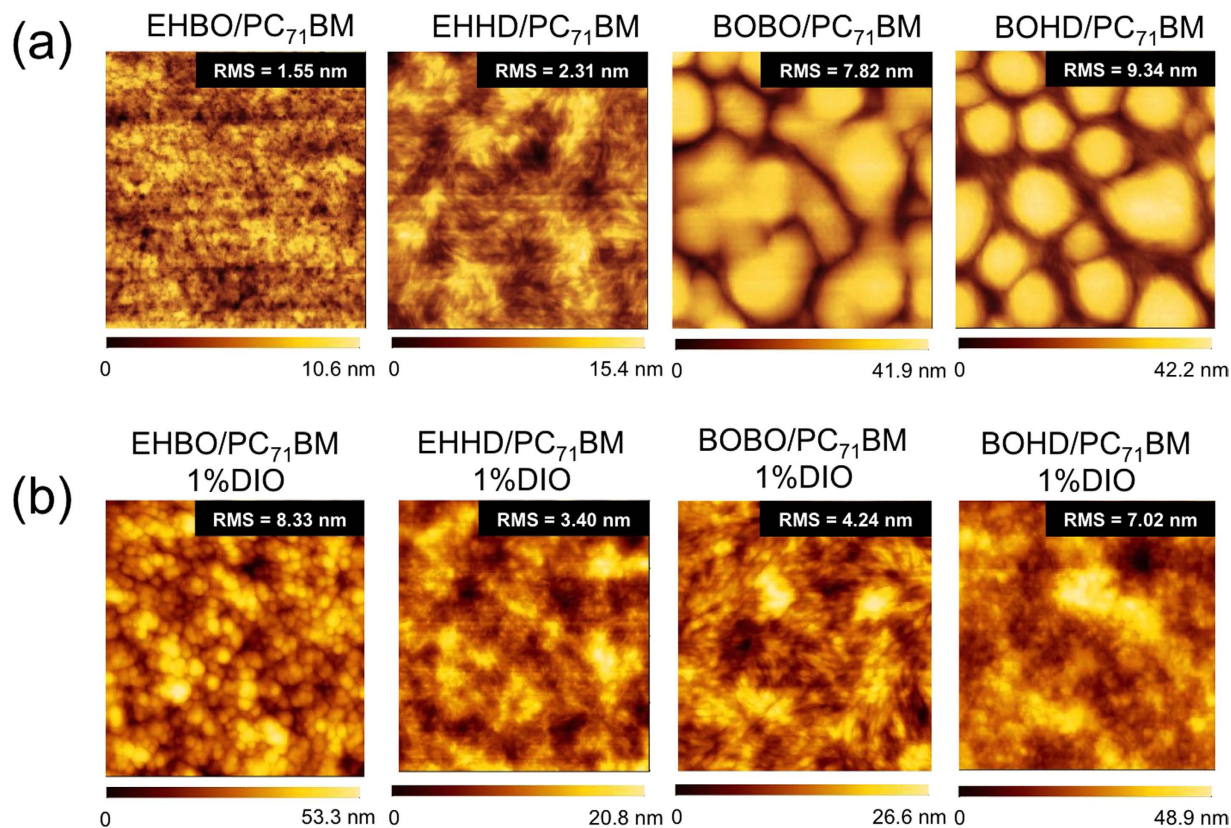
Figure 4. AFM images of PTzNTz/PC$_{71}$BM blend films **(a)** and DIO (1%)-aided PTzNTz/PC$_{71}$BM blend films **(b)**.

spectra. It is found that the fill factor (FF) was higher for the cell using PTzNTz-EHBO (0.67) than those using the other polymers (<0.6). The higher J_{SC} and FF of the PTzNTz-EHBO cell than the others agrees well with the results of the 2D GIXD and AFM studies, as the PTzNTz-EHBO blend film showed a higher crystalline structure and a better phase separated structure than the others when fabricated from CB solutions. As a result, PTzNTz-EHBO cells exhibited PCEs of up to 9.0% (J_{SC} = 16.0 mA cm^{-2}, V_{OC} = 0.84 V, FF = 0.67), and those of the other polymer cells were 1.2–2.1%.

Note that, however, PCEs of the cells using PTzNTz-EHHD, -BOBO and -BOHD were markedly improved when the active layer was fabricated from CB solution including 1% of DIO as the solvent additive (Fig. 5c). In particular, the DIO-aided cells using PTzNTz-EHHD and -BOBO showed significant increase in J_{SC} to ~16.3 and ~15.6 mA cm^{-2}, respectively, which were similar to the value of the cells using PTzNTz-EHBO. The increase in J_{SC} was consistent with the increase in EQE (Fig. 5d). FF was also increased by the addition of DIO to above 0.6 for the PTzNTz-EHHD and -BOBO cells. Thus, PCEs of the cells using these polymers were greatly improved with the association of DIO: 2.1% to 8.8% for PTzNTz-EHHD, 1.7% to 8.8% for PTzNTz-BOBO, and 1.2% to 5.2% for PTzNTz-BOHD (Table 2). PCE of the PTzNTz-EHBO-based cells fabricated with DIO was mostly similar to those without DIO. The improved performances for the cells using these polymers are in good agreement with the changes observed in the 2D GIXD and AFM studies.

We also tested the stability of the cells using PTzNTz-EHBO fabricated with and without DIO and PTzNTz-BOBO fabricated with DIO in comparison with the cells using PTzBT-BOHD. There have been established several procedures for testing device stability based on the consensus reached by the consortia of the international summit on OPV stability (ISOS)[37,38]. In this work, we chose to test our cells in the dark at 85 °C, which refers to category ISOS-D-3[37]. To avoid degradation concerning the encapsulation such as an adhesive material, we tested the cells without encapsulation and stored them on a hotplate in a glovebox. Figure 6a shows the change of PCE as a function of the storage time. PCE of the PTzNTz-EHBO cell decreased gradually from 8.6% to 7.5% after 500 hours, which corresponds to a 13% drop from initial PCE. The DIO-aided PTzNTz-EHBO cell showed similar behavior with a PCE drop of 13%, where PCE decreased from 8.6% to 7.5%, suggesting that DIO does not affect the device stability under these conditions for the PTzNTz system. The DIO-aided PTzNTz-BOBO cell also showed similar behavior with a PCE drop of 13%, where PCE decreased from 8.3% to 7.2%, implying that the effect of the side chain is negligible. In sharp contrast, PCE of the PTzBT-BOHD cell showed a significant drop
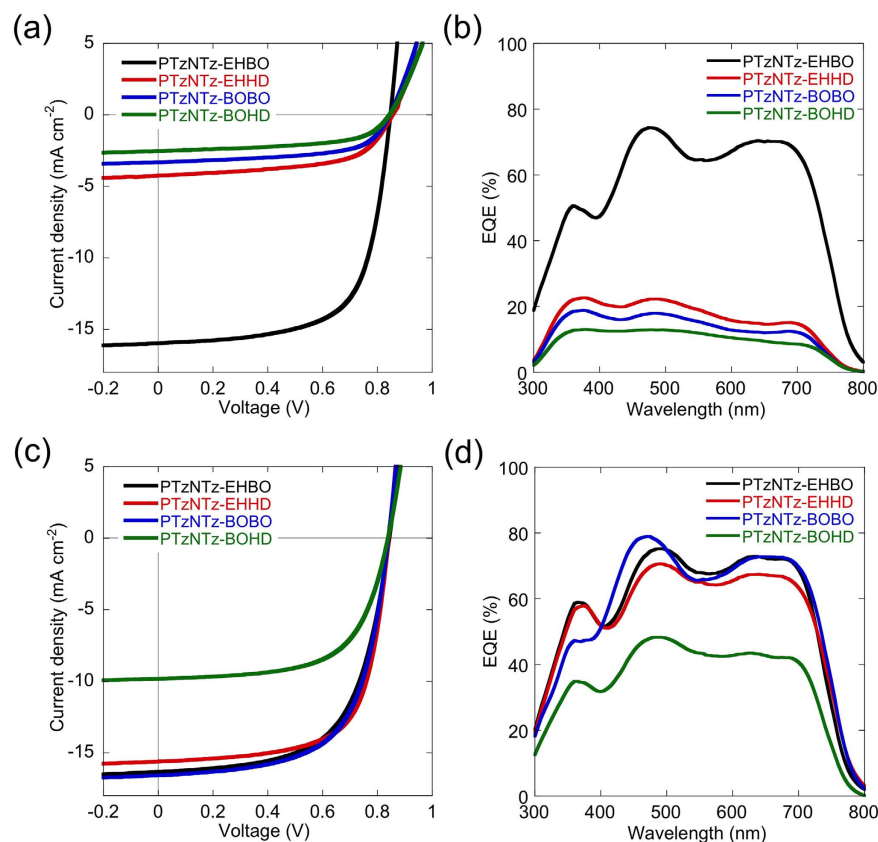
Figure 5. *J–V* curves (a,c) and EQE spectra (b,d) of the solar cells based on PTzNTzs. (**a,b**) The active layer was spun from the CB solution. (**c,d**) The active layer was spun from the CB/DIO (1 v/v%) solution.

Polymer	DIO	J_{SC} (mA cm^{-2})	V_{OC} (V)	FF	PCE$_{max}$ [PCE$_{ave}$] (%)^a
PTzNTz-EHBO	–	16.0	0.84	0.67	9.0 [8.7]
	1%	16.3	0.84	0.62	8.5 [8.1]
PTzNTz-EHHD	–	4.3	0.85	0.58	2.1 [1.9]
	1%	15.6	0.84	0.67	8.8 [8.5]
PTzNTz-BOBO	–	3.3	0.85	0.60	1.7 [1.5]
	1%	16.6	0.84	0.63	8.8 [8.5]
PTzNTz-BOHD	–	2.5	0.84	0.58	1.2 [1.1]
	1%	9.8	0.84	0.63	5.2 [4.8]

Table 2. Photovoltaic properties of the solar cells based on PTzNTzs/PC$_{71}$BM. ^{a}PCE$_{max}$: maximum power conversion efficiencies, PCE$_{ave}$: average power conversion efficiencies.

at the initial stage; PCE decreased from 7.2% to 3.4% after 1 hour, though it showed only a slight degradation thereafter, resulting in an overall drop of 57% after 500 hours. The significant difference in the thermal stability between the PTzNTzs cells and the PTzBT-BOHD cell originates in the difference in V_{OC} and FF (Figure S12), although we do not yet understand the nature of the difference.

Interestingly, when the hole transport layer, MoO$_x$, was replaced with WO$_x$, the thermal stability of the cells were greatly improved (Fig. 6b). All the PTzNTzs cells tested here with the initial PCE of 8.3%, 7.9%, and 7.9% for PTzNTz-EHBO, PTzNTz-EHBO with DIO, and PTzNTz-BOBO with DIO, respectively, showed negligible degradation after 500 hours. The drop of PCE for the PTzBT-BOHD cell was 30% after 500 hours (PCE decreased from 6.8% to 4.8%). The main factor of the stability improvement for the PTzNTzs cells was the improved J_{SC} drop (Figure S12). The improvement in the PTzBT-BOHD cell was mainly due to the improved V_{OC} drop, though J_{SC} was also slightly improved (Figure S12). The difference between the cells with MoO$_x$ and WO$_x$ is currently under investigation. Overall, regardless of
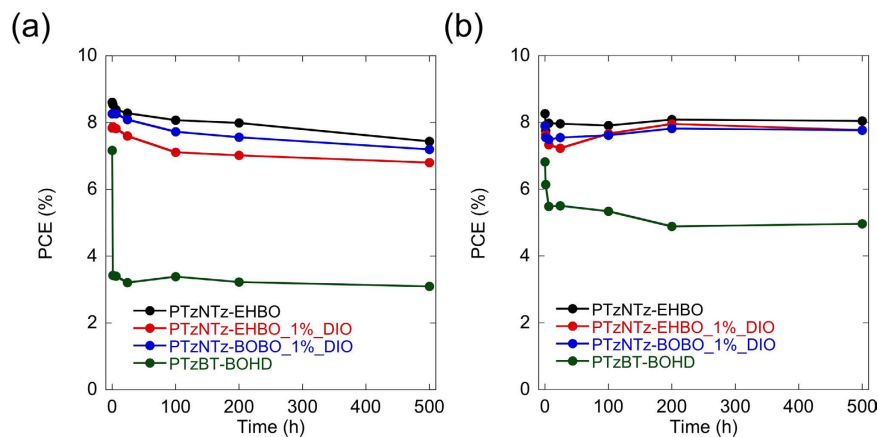
(a) (b)

Figure 6. Change of PCE for the cells using PTzNTz-EHBO fabricated by CB and CB/DIO (1 v/v%), PTzNTz-BOBO fabricated by CB/DIO (1 v/v%), and PTzBT-BOHD fabricated by CB under the storage for 500 hours at 85 °C in the glovebox. MoO_x (**a**) and WO_x (**b**) were used as the hole transport layer of the cells.

the hole transport layer, the PTzNTzs cells are much more stable than the PTzBT-BOHD cell. To date there have been some reports showing the stability of PSCs under various conditions[39–42]. To the best of our knowledge, this is the first report for PSCs to demonstrate such high PCEs of ~9% and almost perfect stability under a standardized conditions at the same time. These results suggest that the introduction of NTz into the polymer backbone is advantageous for the thermal stability of the solar cells as well as PCE.

Conclusion

New thiophene-thiazolothiazole-naphthobisthiadiazole semiconducting polymers (PTzNTzs) were synthesized and characterized, and their photovoltaic characteristics were investigated. The solubility of PTzNTzs were greatly improved from that of PTzBTs. PTzNTzs had both narrow band gaps (ca. 1.57 eV) and low-lying HOMO levels (ca. −5.40 eV) compared to thiophene-thiazolothiazole polymers (PTzBTs) that have been reported before. PTzNTz-EHBO with the shortest side chain combination exhibited the best PCE of as high as 9.0% in the inverted solar cells among the polymers synthesized here. Although the cells based on PTzNTz-BOBO and -EHHD with the longer side chains exhibited very low PCEs of ~2%, the use of DIO at the time of fabrication as the solvent additive greatly improved their PCEs to ~8.8%. The difference of the solar cell behavior between these polymers with different side chain combination is likely attributed to the difference in crystallinity. Interestingly, the PTzNTzs cells demonstrated excellent stability as they showed negligible degradation after 500 hour-storage at 85 °C under N_2 atmosphere. To the best of our knowledge, the PTzNTzs cells are the best performing PSCs in terms of having high PCE and high stability at the same time. These results indicate that PTzNTzs are promising polymers for practical application.

Methods

Materials. 2,5-Bis(3-(2-ethylhexyl-5-(trimethylstannyl)thiophen-2-yl)thiazolo[5,4-*d*]thiazole (**1a**)[28] and 2,5-bis(3-(2-butyloctyl-5-(trimethylstannyl)thiophen-2-yl)thiazolo[5,4-*d*]thiazole (**1b**)[28] 5,10-bis(5-bromo-4-(2-butyloctyl)thiophen-2-yl)naphtho[1,2-*c*:5,6-*c*′]bis[1,2,5]thiadiazole (**2a**)[31] and 5,10-bis(5-bromo-4-(2-hexyldecyl)thiophen-2-yl)naphtho[1,2-c:5,6-c′]bis[1,2,5]thiadiazole (**2b**)[31] were synthesized according to the reported procedure. $Pd(PPh_3)_4$ (PPh_3 = triphenylphosphine) was purchased from Tokyo Chemical Industry, Co., Ltd. (TCI), and used as purchased. Toluene was purified by a Glass Contour Solvent System prior to use. Polymerization was carried out with a microwave reactor, Biotage Initiator. Molecular weight of the polymers was evaluated by a high-temperature GPC (140 °C), TOSOH HLC-8121GPC/HT, using DCB as the eluent and polystyrene standard.

Synthesis of the polymers. To a reaction tube equipped with a stirring bar, the stannylated TzTz monomer (0.10 mmol), the dibrominated NTz monomer (0.10 mmol), $Pd(PPh_3)_4$ (2.3 mg, 0.002 mmol), and CB (5 mL) were added. Then the tube was purged with argon and sealed. The reaction tube was set into a microwave reactor and heated to 180 °C for 40 min. After cooling to room temperature, the reaction solution was poured into 200 mL of methanol containing 5 mL of hydrochloric acid, and stirred for 5 hours. Then the precipitated solid was subjected to the sequential Soxhlet extraction with methanol and hexane, to remove low molecular weight fractions. The residue was then extracted with chloroform for PTzNTz-EHHD, -BOBO, and -BOHD, and CB for PTzNTz-EHBO, and reprecipitated in 200 mL of methanol to yield dark green solid (yield = 68% for PTzNTz-EHBO, 89% for -EHHD, 86% for -BOBO, 75% for -BOHD). Anal. Calcd for $C_{70}H_{92}N_6S_8$ (PTzNTz-EHBO): C, 65.99; H, 7.28; N, 6.60. Found: C,

65.65; H, 7.15; N, 6.31. Calcd for $C_{78}H_{108}N_6S_8$ (-EHHD): C, 67.58; H, 7.85; N, 6.06. Found: C, 67.64; H, 7.80; N, 5.93. Calcd for $C_{78}H_{108}N_6S_8$ (-BOBO): C, 67.58; H, 7.85; N, 6.06. Found: C, 67.62; H, 7.74; N, 5.98. Calcd for $C_{86}H_{124}N_6S_8$ (-BOHD): C, 68.93; H, 8.34; N, 5.61. Found: C, 68.55; H, 8.20; N, 5.45.

Solar Cell Fabrication and Measurement. Patterned ITO substrates (purchased from Atsugi Micro) were first pre-cleaned sequentially by sonicating in a detergent bath, de-ionized water, acetone, and isopropanol at rt, and in boiled isopropanol each for 10 min, and then baked at 120 °C for 10 min in air. The substrates were then subjected to a UV/ozone treatment at rt for 20 min. ZnO layer was prepared by spin-coating (at 5000 rpm, 30 sec) a precursor solution prepared from zinc acetate dehydrate (0.5 g) and ethanolamine (0.14 mL) in 5 mL of 2-methoxyethanol. ZnO substrates were immediately baked at 200 °C for 30 min in air, and then rinsed with acetone, isopropanol and boiled isopropanol for 10 min. The photoactive layer was deposited in a glove box (KOREA KIYON, KK-011AS-EXTRA) by spin coating. CB solution containing 5~7 g/L of the polymer sample with respective amount of $PC_{71}BM$ was kept at 100 °C for 30 min. The hot CB solution was directly spin-coated on the substrate at 600 rpm for 20 sec. The thin films were transferred into a vacuum evaporator (ALS Technology, E-100J) connected to the glove box, and the MoO_x layer (7.5 nm) or WO_x layer (15 nm) was deposited, followed by the deposition of the Ag layer (100 nm). The active area of the cells was 0.16 cm^2. J–V characteristics of the cells were measured using a Keithley 2400 source-measure unit in nitrogen atmosphere under 1 sun (AM1.5 G) conditions using a solar simulator (SAN-EI Electric, XES-40S1). The light intensity was calibrated with a reference PV cell (KONICA MINOLTA AK-100 certified at National Institute of Advanced Industrial Science and Technology, Japan). EQE spectra were measured with a Spectral Response Measuring System (SOMA OPTICS, S-9241). More than 10 different devices were made and measured to collect the photovoltaic properties. For thermal stability tests, cells were stored on a hotplate at 85 °C in the glovebox. J–V characteristics were measured after 1, 2, 6, 24, 100, 200 and 500 hours.

References

1. Yu, G., Gao, J., Hummelen, J. C., Wudl, F. & Heeger, A. J. Polymer photovoltaic cells: enhanced efficiencies via a network of internal donor-acceptor heterojunctions. *Science* **270,** 1789–1791 (1995).
2. Günes, S., Neugebauer, H. & Sariciftci, N. S. Conjugated polymer-based organic solar cells. *Chem. Rev.* **107,** 1324–1338 (2007).
3. Christoph, B. & Scherf. U. *Organic photovoltaics: materials, device physics, and manufacturing technologies.* (2008).
4. Liang, Y. *et al.* For the bright future-bulk heterojunction polymer solar cells with power conversion efficiency of 7.4%. *Adv. Mater.* **22,** E135–138 (2010).
5. Chen, H.-C. *et al.* Prominent short-circuit currents of fluorinated quinoxaline-based copolymer solar cells with a power conversion efficiency of 8.0%. *Chem. Mater.* **24,** 4766–4772 (2012).
6. Cabanetos, C. *et al.* Linear side chains in benzo[1,2-b:4,5-b']dithiophene-thieno[3,4-c]pyrrole-4,6-dione polymers direct self-assembly and solar cell performance. *J. Am. Chem. Soc.* **135,** 4656–4659 (2013).
7. Osaka, I., Kakara, T., Takemura, N., Koganezawa, T. & Takimiya, K. Naphthodithiophene-naphthobisthiadiazole copolymers for solar cells: alkylation drives the polymer backbone flat and promotes efficiency. *J. Am. Chem. Soc.* **135,** 8834–8837 (2013).
8. Ye, L., Zhang, S., Zhao, W., Yao, H. & Hou, J. Highly efficient 2D-conjugated benzodithiophene-based photovoltaic polymer with linear alkylthio side chain. *Chem. Mater.* **26,** 3603–3605 (2014).
9. Peet, J. *et al.* Efficiency enhancement in low-bandgap polymer solar cells by processing with alkane dithiols. *Nature Mater.* **6,** 497–500 (2007).
10. He, Z. *et al.* Enhanced power-conversion efficiency in polymer solar cells using an inverted device structure. *Nat. Photon.* **6,** 593–597 (2012).
11. Liao, S. H. *et al.* Single junction inverted polymer solar cell reaching power conversion efficiency 10.31% by employing dual-doped zinc oxide nano-film as cathode interlayer. *Sci. Rep.* **4,** 6813 (2014).
12. Liu, Y. *et al.* Aggregation and morphology control enables multiple cases of high-efficiency polymer solar cells. *Nat. Commun.* **5,** 5293 (2014).
13. Vohra, V. *et al.* Effect inverted polymer solar cells employing favourable molecular orientation. *Nat. Photon.* **9,** 403–408 (2015).
14. Guo, J. *et al.* Structure, dynamics, and power conversion efficiency correlations in a new low bandgap polymer: PCBM solar cell. *J. Phys. Chem. B* **114,** 742–748 (2010).
15. Scharber, M. C. *et al.* Design rules for donors in bulk-heterojunction solar cells—towards 10% energy-conversion efficiency. *Adv. Mater.* **18,** 789–794 (2006).
16. Thompson, B. C. & Frechet, J. M. Polymer-fullerene composite solar cells. *Angew. Chem. Int. Ed.* **47,** 58–77 (2008).
17. Facchetti, A. π-conjugated polymers for organic electronics and photovoltaic cell applications. *Chem. Mater.* **23,** 733–758 (2011).
18. Boudreault, P.-L. T., Najari, A. & Leclerc, M. Processable low-bandgap polymers for photovoltaic applications. *Chem. Mater.* **23,** 456–469 (2011).
19. Beaujuge, P. M. & Frechet, J. M. Molecular design and ordering effects in pi-functional materials for transistor and solar cell applications. *J. Am. Chem. Soc.* **133,** 20009–20029 (2011).
20. Wu, J. S., Cheng, S. W., Cheng, Y. J. & Hsu, C. S. Donor-acceptor conjugated polymers based on multifused ladder-type arenes for organic solar cells. *Chem. Soc. Rev.* **44,** 1113–1154 (2015).
21. Ando, S. *et al.* High performance n-type organic field-effect transistors based on π-electronic systems with trifluoromethylphenyl groups. *J. Am. Chem. Soc.* **27,** 5336–5337 (2005).
22. Osaka, I., Sauvé, G., Zhang, R., Kowalewski, T. & McCullough, R. D. Novel thiophene-thiazolothiazole copolymers for organic field-effect transistors. *Adv. Mater.* **19,** 4160–4165 (2007).
23. Osaka, I. *et al.* High-lamellar ordering and amorphous-like π-network in short-chain thiazolothiazole−thiophene copolymers lead to high mobilities. *J. Am. Chem. Soc.* **131,** 2521–2529 (2009).
24. Osaka, I. *et al.* Highly stable semiconducting polymers based on thiazolothiazole. *Chem. Mater.* **22,** 4191–4196 (2010).
25. Meiss, J. *et al.* Highly efficient semitransparent tandem organic solar cells with complementary absorber materials. *Appl. Phys. Lett.* **99,** 043301 (2011).
26. Subramaniyan, S. *et al.* Effects of side chains on thiazolothiazole-based copolymer semiconductors for high performance solar cells. *Adv. Energy Mater.* **1,** 854–860 (2011).

27. Osaka, I., Saito, M., Mori, H., Koganezawa, T. & Takimiya, K. Drastic change of molecular orientation in a thiazolothiazole copolymer by molecular-weight control and blending with PC$_{61}$BM leads to high efficiencies in solar cells. *Adv. Mater.* **24,** 425–430 (2012).
28. Osaka, I., Saito, M., Koganezawa, T. & Takimiya, K. Thiophene-thiazolothiazole copolymers: significant impact of side chain composition on backbone orientation and solar cell performances. *Adv. Mater.* **26,** 331–338 (2014).
29. Mataka, S. *et al.* Sulfur nitride in organic chemistry. part 19. selective formation of benzo- and benzobis[1,2,5]thiadiazole skeleton in the reaction of tetrasulfur tetranitride with naphthalenols and related compounds. *Bull. Chem. Soc. Jap.* **64,** 68–73 (1991).
30. Wang, M. *et al.* Donor-acceptor conjugated polymer based on naphtho[1,2-*c*:5,6-*c′*]bis[1,2,5]thiadiazole for high-performance polymer solar cells. *J. Am. Chem. Soc.* **133,** 9638–9641 (2011).
31. Osaka, I. *et al.* Synthesis, characterization, and transistor and solar cell applications of a naphthobisthiadiazole-based semiconducting polymer. *J. Am. Chem. Soc.* **134,** 3498–3507 (2012).
32. Osaka, I., Abe, T., Shimawaki, M., Koganezawa, T. & Takimiya, K. Naphthodithiophene-based donor–acceptor polymers: versatile semiconductors for OFETs and OPVs. *ACS Macro Lett.* **1,** 437–440 (2012).
33. Takimiya, K., Osaka, I. & Nakano, M. π-Building blocks for organic electronics: revaluation of "inductive" and "resonance" effects of π-electron deficient units. *Chem. Mater.* **26,** 587–593 (2014).
34. Rivnay, J., Mannsfeld, S. C., Miller, C. E., Salleo, A. & Toney, M. F. Quantitative determination of organic semiconductor microstructure from the molecular to device scale. *Chem. Rev.* **112,** 5488–5519 (2012).
35. Lee, J. K. *et al.* Processing additives for improved efficiency from bulk heterojunction solar cells. *J. Am. Chem. Soc.* **130,** 3619–3623 (2008).
36. Lou, S. J. *et al.* Effects of additives on the morphology of solution phase aggregates formed by active layer components of high-efficiency organic solar cells. *J. Am. Chem. Soc.* **133,** 20661–20663 (2011).
37. Reese, M. O. *et al.* Consensus stability testing protocols for organic photovoltaic materials and devices. *Sol. Energy Mater. Sol. Cells* **95,** 1253–1267 (2011).
38. Tanenbaum, D. M. *et al.* The ISOS-3 inter-laboratory collaboration focused on the stability of a variety of organic photovoltaic devices. *RSC Adv.* **2,** 882–893 (2012).
39. Neugebauer, H. *et al.* Stability and photodegradation mechanisms of conjugated polymer/fullerene plastic solar cells. *Sol. Energy Mater. Sol. Cells* **61,** 35–42 (2000).
40. Lloyd, M. T. *et al.* Impact of contact evolution on the shelf life of organic solar cells. *J. Mater. Chem.* **19,** 7638–7642 (2009).
41. Peters, C. H. *et al.* High efficiency polymer solar cells with long operating lifetimes. *Adv. Energy Mater.* **1,** 491–494 (2011).
42. Kesters, J. *et al.* Enhanced organic solar cell stability by polymer (PCPDTBT) side chain functionalization. *Chem. Mater.* **27,** 1332–1341 (2015).

Acknowledgements

Author Contributions

I.O. designed and directed the project. M.S. and Y.S. synthesized the polymers. M.S. conducted the measurements for the polymer properties, thin film analyses, and device fabrication and measurements. M.S. conducted the stability tests for the devices with the support of T.O., S.I., T.A. and M.S. wrote the initial draft of the manuscript, and I.O. wrote the final draft of the manuscript. K.T., T.O., S.I. and T.A. were involved in the discussion. All authors reviewed the manuscript.

Additional Information

Supplementary information accompanies this paper at http://www.nature.com/srep

Competing financial interests: The authors declare no competing financial interests.

How to cite this article: Saito, M. *et al.* Highly Efficient and Stable Solar Cells Based on Thiazolothiazole and Naphthobisthiadiazole Copolymers. *Sci. Rep.* **5**, 14202; doi: 10.1038/srep14202 (2015).